Multiple Ionization of Ne, Ar, and Kr Produced by X Rays in the Energy Range 0.28–8.03 keV*

G. S. Lightner,† R. J. Van Brunt, and W. D. Whitehead
University of Virginia, Charlottesville, Virginia 22901
(Received 2 March 1971)

Relative abundances of multiply charged neon, argon, and krypton ions produced by x rays of energies 0.28, 1.5, 5.4, and 8.0 keV have been measured with a time-of-flight mass spectrometer. Effectively monoenergetic x rays were obtained by a filtering technique whereby two filters with transmissions matching at all energies except at the K characteristic line of the x-ray tube target material were alternately placed in the x-ray beam. The data when corrected for charge-dependent discrimination effects are consistent with previous measurements and, except for neon, with calculations which include the electron shakeoff mechanism in addition to Auger transitions. The results for neon at 0.28 keV confirm the need for including electron correlation effects in the description of the ionization process. Other discrepancies between theory and experiment can be explained by considering the energy dependence of partial photoionization cross sections calculated by Rakavy and Ron.

I. INTRODUCTION

Previous investigations of multiple ionization of rare gases have demonstrated that Auger transitions[1] following inner-shell ionization do not completely account for the observed relative abundances of the various ions.[2–10] In some cases considerably more ionization is observed than is predicted from Auger transitions. Most of this additional ionization can be accounted for by electron shakeoff in which an outer-shell electron is excited to the continuum by the sudden change in atomic potential following creation of an inner-shell vacancy.[2,11] Recent calculations for helium and neon[12–14] which employ correlated wave functions demonstrate that correlation effects may also be of significance in the production of doubly charged ions.

The purpose of this work is to investigate existing discrepancies between theory and observation of the relative abundances of multiply charged ions produced by photoionization in the soft x-ray region which are possibly due to errors in the partial photoionization cross sections used to obtain the theoretical values and to the relatively wide energy spectra of the x rays often used to produce the ionization. In the present experiment, new measurements of the relative abundances of multiply charged neon, argon, and krypton ions were made using a balanced filter technique to effectively obtain monoenergetic ionizing x rays. It is shown that by the use of a more precisely defined x-ray energy coupled with interpretation which considers recently calculated partial photoionization cross sections,[15,16] it is possible to remove some of the ambiguities and uncertainties connected with the disagreements between theory and experiment.

II. EXPERIMENT

The total ion yield Y obtained in a photoionization experiment can be represented by

$$Y = K \int_0^{E_0} \frac{dN(E, E_0)}{dE} \sigma(E)\, dE \ , \tag{1}$$

where dN/dE is the number of photons with energy between E and $E+dE$, σ is the photoelectric cross section, E_0 is the maximum energy of the photons, and K is a factor which includes the geometry, collection efficiency, target gas pressure, x-ray tube current, and collection time. The yield for a given ion of charge c is

$$Y_c = K_c \int_0^{E_0} \frac{dN(E, E_0)}{dE} \rho_c(E)\, dE \ , \tag{2}$$

where $\rho_c(E)$ is the cross section for creating an ion of final charge c as a function of photon energy. If the final charge state results from a two-step process, whereby direct ionization by the incident photon is followed by a reorganization that proceeds with fixed probability to one of the possible final charge states, then the yield can be written as

$$Y_c = K_c \sum_i \int_{E_i}^{E_0} \frac{dN(E, E_0)}{dE} \alpha_i^c \sigma_i(E)\, dE \ , \tag{3}$$

where the sum is over all atomic sublevels i, $\sigma_i(E)$ is the cross section for electron removal from the ith sublevel, α_i^c is the probability that an ion of charge c is created from electronic rearrangement when a vacancy exists in the ith sublevel, and E_i is the ionization threshold energy for this level. The relative yield is the ratio of Eq. (2) to Eq. (1). The interpretation of this ratio is simplified if the x-ray spectrum is monoenergetic, thus allowing it to be represented by a δ function:

$$\frac{dN}{dE} = N_0\, \delta(E - E_k) \ ,$$

which gives for the relative yields

$$\frac{Y_c}{Y}=\frac{K_c}{K}\,\frac{\sum_i N_0\,\alpha_i^c\sigma_i(E_k)}{N_0\sigma(E_k)}\ . \qquad (4)$$

The ratio K_c/K is unity if there are no charge-dependent instrumental effects.

An effectively monoenergetic x-ray beam was obtained by a balanced filter technique first used by Ross[17] in which two filters were alternately placed in the x-ray beam, one with a K absorption edge above, the other below the x-ray energy of interest corresponding to the K characteristic line of the target material. The transmissions of the filters were matched everywhere except at the energy of interest and the resulting difference in ion count with these filters corresponded essentially to the monoenergetic K line of the target. Figure 1 shows typical calculated transmission curves for the pair of matched filters, 15.7-μ magnesium and 8.6-μ aluminum.[18] The transmissions match everywhere except in the region of the 1.5-keV K characteristic lines of the aluminum target, so that the difference in ion count rate obtained with these filters is mainly due to photons of this energy. Since the filters are matched at the higher energies, the x-ray tube may be operated at as a high a voltage possible to maximize the intensity of the target characteristic lines. Table I indicates the target and filter combinations used in the present work. The $K\alpha$ and $K\beta$ lines for carbon and aluminum targets and the $K\alpha$ lines for chromium and copper targets fall between the limits defined by the K absorption edges of the two filters. Also shown in the table are the filter thicknesses used with their estimated uncertainties. The values for the mass absorption coefficients used to calculate the filter transmissions may be in error by as much as 10% in some cases.[18]

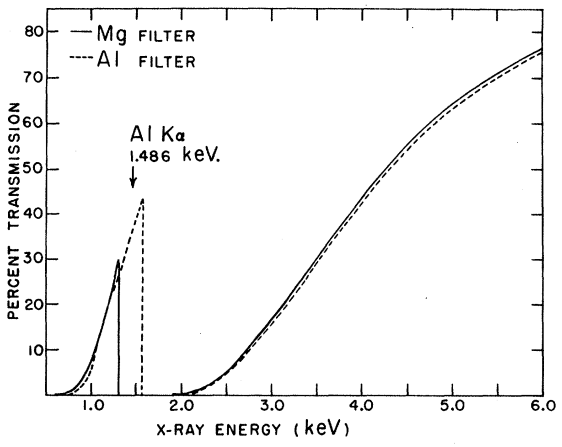

FIG. 1. Transmission curves for matched 8.6-μ aluminum and 15.7-μ magnesium x-ray filters used to isolate the K characteristic line of aluminum calculated using mass absorption coefficients tabulated in Ref. 18.

Charge analysis of the ions was accomplished with a pulsed linear time-of-flight (TOF) mass spectrometer similar in design to that of Wiley and McLaren.[19] The operating characteristics of the instrument used have previously been described in detail.[20,21] By using a pulsed x-ray beam, disadvantages associated with coincidence techniques previously used for timing[2] were eliminated, while the advantage of collecting all ions under identical experimental conditions was retained.

Figure 2 shows a schematic diagram of the experimental arrangement. Radiation from a pulsed x-ray tube (1) was collimated (2) and filtered (3) before entering the ionization region between grids G2 and G3. An x-ray trap (4) was used to monitor the beam intensity and to suppress secondary electrons. Two of the four slits in the collimator were also used as secondary-electron suppressors. By use of appropriate voltages on G1, G2, and G3, ions were trapped in the ionization region between G2 and G3 while the x-ray beam was on. The choice of bias voltages was based on achieving maximum count rate with minimum charge discrimination.[21,22]

After the x-ray pulse was turned off, a positive 52-V pulse was applied to G2 to push the ions into the region between G3 and G4, where they were accelerated through a potential difference of -1520 V before entering the linear drift tube (5). The drift tube was made of 2.5-in. copper tubing which was 210.64 cm in length. Detection, following flight times on the order of 15 μsec, was achieved by a Bendix model 306 magnetic electron multiplier (6). A timing start pulse, coincident with the pusher pulse, and the ion detector pulse triggered, respectively, the start and stop of a time-to-amplitude converter, the output of which was fed to a 512-channel multichannel pulse-height analyzer. Only one ion could therefore be detected per x-ray pulse.

For all measurements the x-ray tube was operated at 20 kV with a pulse current of 100 mA at a frequency of 10 kHz. The x-ray pulse width was always 2 μsec full width at half-maximum.[22] It was demonstrated from pressure dependence measurements that at the gas pressures used (4×10^{-5} Torr for neon, 5×10^{-5} Torr for argon, and 7×10^{-5} Torr for krypton), charge-exchange collisions in the ion source were negligible.

Because of the low count rates (from 0.5 to 24 counts/min, depending on the target-gas combination), data were accumulated over long periods of time. The matched filters were mounted on a movable vacuum feedthrough and interchanged once every 4–10 min. The ion count for each filter was accumulated in separate sections of the multichannel analyzer. The total count for each ion charge included a summation over all observed isotopes of

TABLE I. Target and filter combinations used to obtain a monoenergetic x-ray beam. The numbers in parentheses give the positions of the K absorption edges for the filters in keV which define the limits of the effective x-ray window. Also indicated are the filter thicknesses in microns.

Target material	K line (keV)	Filters			
		K edge	Thickness	K edge	Thickness
C	0.28	Mylar (0.284)	6.3±0.3	Be (0.19)	26 ±1
Al	1.5	Al (1.560)	8.6±0.3	Mg (1.303)	15.7±0.3
Cr	5.4	V (5.464)	12.2±0.5	Ti (4.956)	19.3±0.8
Cu	8.0	Ni (8.332)	10.2±0.3	Co (7.709)	11.2±0.3

the atomic species.

III. RESULTS AND DISCUSSION

A. Data

The measured relative abundances of neon, argon, and krypton ions at different x-ray energies are shown in Tables II–VII. No measurements were made at 8.0 keV for neon. The errors shown merely represent the counting statistics for the total accumulated data, which were obtained over a period of several days. Reproducibility of ion charge spectra from day to day was generally within the counting statistics, although, as judged from the range of values, the errors could be as much as an additional 5% higher. Reproducibility of the data was determined largely by the stability of the instrument and operating conditions during the period that the two different filters were in the x-ray beam.

Several charge-dependent instrumental discrimination effects were considered as possible sources of error. One due to motion of the ions in the ionization region prior to application of the extraction pulse was largely overcome by applying the appropriate voltages to the grids of the ion source.[21] Calculation of ion losses due to this motion for the grid voltages used indicated that collection efficiency for each charge was the same within an estimated error of 3%. The largest error due to this effect is associated with the results for krypton.

In this experiment charge discrimination also resulted from a geometric effect due to the finite size of the detector and the transverse motion of the ions resulting from their initial energy (thermal plus recoil).[21] Because the size of the detector aperture was smaller than the estimated extent of the ion beam in the plane of the detector, some of the ions which entered the drift tube could not be detected. Figure 3 shows calculated ion collection efficiencies due to this effect for the various ion charges as a function of the initial kinetic energies for the present experimental conditions.[21] The resulting collection efficiency is lowest for ions of lowest charge.

The data corrected for collection efficiency are shown in the tables, with the mean initial energy value used shown in parentheses in the column heading. The errors in this correction are associated with uncertainties in the ion recoil energy and pos-

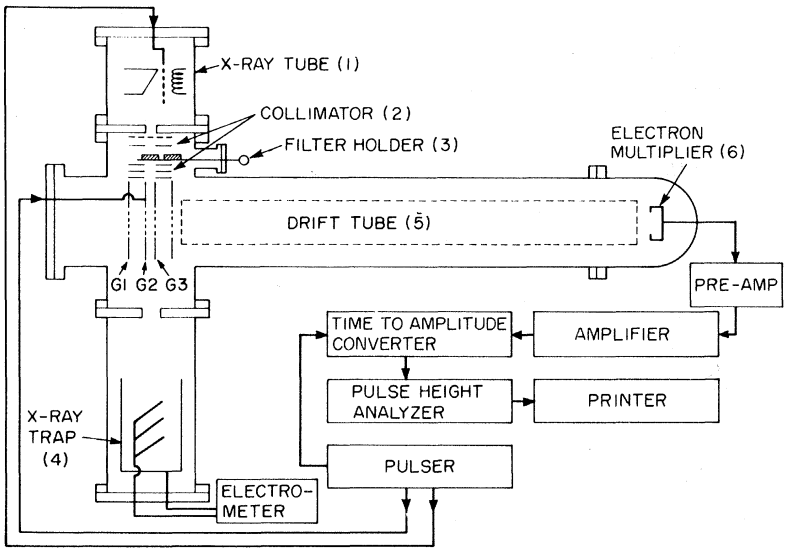

FIG. 2. Time-of-flight mass analyzer.

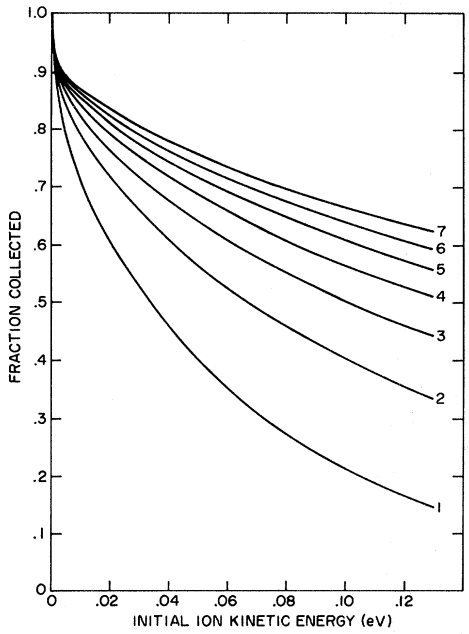

FIG. 3. Calculated percentage of the total number of ions initially entering the drift tube which also enter the detector as a function of initial ion kinetic energy (thermal plus recoil) and charge. The details of this calculation are described in Ref. 21.

sible small effects due to the presence of electric and magnetic fields near the detector. The errors are consequently expected to be higher for those cases involving the largest recoil. This correction also does not allow for possible small effects which might result from variation in ion detection efficiency as a function of the ion impact position on the detector.[23]

Another source of possible charge-dependent discrimination is associated with detector response. A measurement of the ion detection efficiency of the multiplier indicated a small decrease in detection efficiency with decreasing ion charge, and therefore ion impact velocity, consistent with earlier observations.[22,24] The greatest observed difference in efficiency was about 5%, although there was an estimated uncertainty of 6% associated with these measurements. Corrections for this effect have not been applied to the data.

B. Interpretation of Results

For neon photoionized by 0.28-keV x rays, only outer-shell ionization is possible and Auger transitions are not energetically allowed. As seen in Table II, our corrected results agree well with two earlier experiments by Carlson[4] in which the average x-ray energy was assumed to be 0.225 keV. The experimental results indicate a greater degree of multiple ionization (14% Ne^{+2}) than the shakeoff theory predicts, as shown in column 4 of Table II, where the theoretical values were also obtained from Carlson.[4] Our experimental results confirm the need for a better theoretical calculation, which possibly includes correlated wave functions to estimate the contribution of double ionization.[14]

The 1.5- and 5.4-keV x rays are capable of ionizing neon in the K shell. Comparisons are made with data from previous experiments in which x rays from an aluminum target ($K\alpha$ energy = 1.49 keV, column 4 of Table III) and a titanium target ($K\alpha$ energy = 4.5 keV, column 7 of Table III) were used.[5] Also included are comparisons with calculated values (column 8, Table III) in which only Auger transitions and electron shakeoff were included. These values were interpreted from Table III of Carlson and Krause,[5] where we used their estimate that Ne^{+} constitutes 6.5% of the ions formed. Our work is in good agreement with both the previous experiments and the calculation. The similarity of the results at 1.5 and 5.4 keV suggests that the relative ionization and rearrangement probabilities [(σ_i/σ)'s and α_i^c's of Eq. (4)] are independent of the incident photon energy in this range, which is expected since the requirements for the sudden approximation used to predict electron shakeoff are satisfied, and no new electronic subshells are available for ionization.

The argon ion spectrum due to the 0.28-keV x rays (Table IV) is particularly interesting because this energy falls between the 2s and 2p levels of argon. As judged from the L/M edge jump of the

TABLE II. Relative abundances of neon ions following ionization by 0.28-keV x rays. Comparison with previous experiment and theory.

Charge of ion (c)	Y_c/Y Uncorrected	Corrected (0.05 ± 0.02 eV)	Previous experiments[a] I	II	Theory[a]
1	0.788 ± 0.014	0.842 ± 0.025	0.870 ± 0.03	0.857	0.955
2	0.189 ± 0.008	0.144 ± 0.015	0.122 ± 0.005	0.138	0.045
3	0.020 ± 0.004	0.013 ± 0.003	0.007 ± 0.001		
4	0.001 ± 0.001	0.001 ± 0.001			
5	0.000 ± 0.001				

[a]Reference 4; I, from measurements of ion abundances; II, from measurements of ejected electrons.

TABLE III. Relative abundances of neon ions following ionization by 1.5- and 5.4- keV x rays. Comparison with previous experiment and theory.

	1.5 keV Y_c/Y			5.4 keV Y_c/Y			
Charge of ion (c)	Uncorrected	Corrected (0.06 ± 0.02 eV)	Previous experiment[a]	Uncorrected	Corrected (0.07 ± 0.03 eV)	Previous experiment[a]	Theory[b]
1	0.041 ± 0.002	0.062 ± 0.010	0.057 ± 0.006	0.055 ± 0.008	0.088 ± 0.01	0.08 ± 0.02	0.065
2	0.685 ± 0.012	0.698 ± 0.013	0.702 ± 0.005	0.685 ± 0.035	0.695 ± 0.038	0.69 ± 0.02	0.703
3	0.235 ± 0.006	0.207 ± 0.008	0.208 ± 0.003	0.221 ± 0.018	0.190 ± 0.020	0.195 ± 0.02	0.202
4	0.037 ± 0.002	0.030 ± 0.002	0.030 ± 0.002	0.036 ± 0.007	0.027 ± 0.008	0.035 ± 0.008	0.027
5	0.003 ± 0.001	0.002 ± 0.001	0.003 ± 0.001	0.004 ± 0.002	0.003 ± 0.002	...	0.003

[a]Reference 5.

[b]Obtained by combining α_i^c's with σ_i from Ref. 5 in the manner of Eq. (4).

argon photoelectric cross section,[25] about 6% of the ionization occurs in the M level and 94% in the $2p$ level. A previous experiment[3,4] indicates that 16% of the ions resulting from outer-shell ionization of argon will be Ar^{+2}, which for this case represents at most 1% of the total number of doubly charged ions. Likewise, the number of Ar^+ ions following ionization in the $2p$ level will be negligible since the probabilities for competing radiative transitions are very small.[6] It is therefore reasonable to assume all Ar^+ ions to be the consequence of M-level ionization, and all multiply charged ions to be the consequences of $2p$ ionization. The ion abundances relative to the total number of multiply charged ions formed are then simply given by the relative probabilities (α_{2p}^c's) for producing an ion with charge c following an initial $2p$ vacancy. These probabilities are compared directly with values obtained by using Auger transition probabilities and electron shakeoff theory[6] as shown in Table IV. In this case there appears to be acceptable agreement.

For 1.5-keV x rays, ionization can occur in the $2s$, $2p$, and $3s$ levels of argon. The values obtained are compared with those of a similar experiment by Carlson and Krause[5] (Table V). The observed ion abundances in this case do not agree with the theoretical abundances calculated by combining relative photoionization cross sections obtained from the modified Stobbe-Hall formula[5,26] and α_i^c's (including the α_{2p}^c's used to explain the 0.28-keV data) in the manner of Eq. (4). The agreement between theory and experiment at 0.28 keV suggests that reasonable values for the α_{2p}^c's have been calculated. This, coupled with the fact that the present experimental data at 1.5 keV confirm former experimental results, suggests that the discrepancy may be largely due to the choice of partial photoionization cross sections. Interpolation of partial cross sections for aluminum and iron calculated by Rakavy and Ron[15] using modified Fermi-Amaldi atomic potentials implies that the $2p$ cross section in argon should be larger than the $2s$ cross section, which is the opposite of values calculated by Carlson and Krause from the Stobbe-Hall approximation. This would tend to bring the theoretical prediction into better agreement with experiment, since the theoretical value for the Ar^{+3}-to-Ar^{+2} abundance ratio is higher than the experimental values. This change, however, would increase a smaller discrepancy in the Ar^{+4} and Ar^{+7} abundances, suggesting a possible small error in the

TABLE IV. Relative abundances of argon ions following ionization by 0.28- and 1.5-keV x rays. Comparison with previous experiment and theory.

	0.28 keV				1.5 keV		
	Y_c/Y		$Y_c \Big/ \sum_2^4 Y_c$		Y_c/Y		
Charge of ion (c)	Uncorrected	Corrected (0.05 ± 0.01 eV)	(corrected)	Theory[a]	Uncorrected	Corrected (0.05 ± 0.01 eV)	Previous experiment[b]
1	0.050 ± 0.004	0.070 ± 0.010			0.043 ± 0.004	0.064 ± 0.008	0.044 ± 0.015
2	0.800 ± 0.018	0.797 ± 0.020	0.856 ± 0.021	0.870	0.410 ± 0.012	0.434 ± 0.014	0.470 ± 0.011
3	0.144 ± 0.006	0.127 ± 0.008	0.136 ± 0.009	0.119	0.410 ± 0.012	0.383 ± 0.013	0.370 ± 0.009
4	0.008 ± 0.002	0.007 ± 0.002	0.008 ± 0.002	0.010	0.110 ± 0.006	0.096 ± 0.007	0.093 ± 0.006
5					0.025 ± 0.004	0.021 ± 0.004	0.019 ± 0.004
6					0.002 ± 0.002	0.002 ± 0.002	0.004 ± 0.002
7					0.001 ± 0.001	0.001 ± 0.001	

[a]Reference 6.

[b]Reference 5.

TABLE V. Relative abundances of argon ions following ionization by 5.4- and 8.0-keV x rays. Comparisons with previous experiment and theory.

	5.4 keV				8.0 keV		
	Y_c/Y				Y_c/Y		
Charge of ion (c)	Uncorrected	Corrected (0.05 ± 0.02 eV)	Previous experiment[a]	Theory[a]	Uncorrected	Corrected (0.05 ± 0.02 eV)	Theory[b]
1	0.025 ± 0.004	0.042 ± 0.006	0.020 ± 0.01	0.014	0.014 ± 0.016	0.024 ± 0.024	0.015
2	0.073 ± 0.007	0.087 ± 0.008	0.104 ± 0.005	0.107	0.061 ± 0.019	0.074 ± 0.022	0.100
3	0.132 ± 0.009	0.139 ± 0.010	0.135 ± 0.005	0.143	0.127 ± 0.026	0.134 ± 0.028	0.136
4	0.351 ± 0.016	0.344 ± 0.016	0.352 ± 0.008	0.399	0.341 ± 0.043	0.339 ± 0.043	0.400
5	0.280 ± 0.013	0.263 ± 0.013	0.259 ± 0.008	0.230	0.300 ± 0.036	0.285 ± 0.036	0.230
6	0.109 ± 0.008	0.099 ± 0.008	0.099 ± 0.007	0.094	0.123 ± 0.022	0.113 ± 0.021	0.094
7	0.026 ± 0.004	0.023 ± 0.004	0.027 ± 0.005	0.022	0.032 ± 0.010	0.029 ± 0.010	0.022
8	0.003 ± 0.002	0.003 ± 0.002	0.004 ± 0.002	0.005	0.002 ± 0.005	0.002 ± 0.005	0.005

[a]Reference 5; 4.5-keV x rays were used.

[b]Obtained by combining α_i^c's from Ref. 5 with interpolated σ_i from Ref. 15.

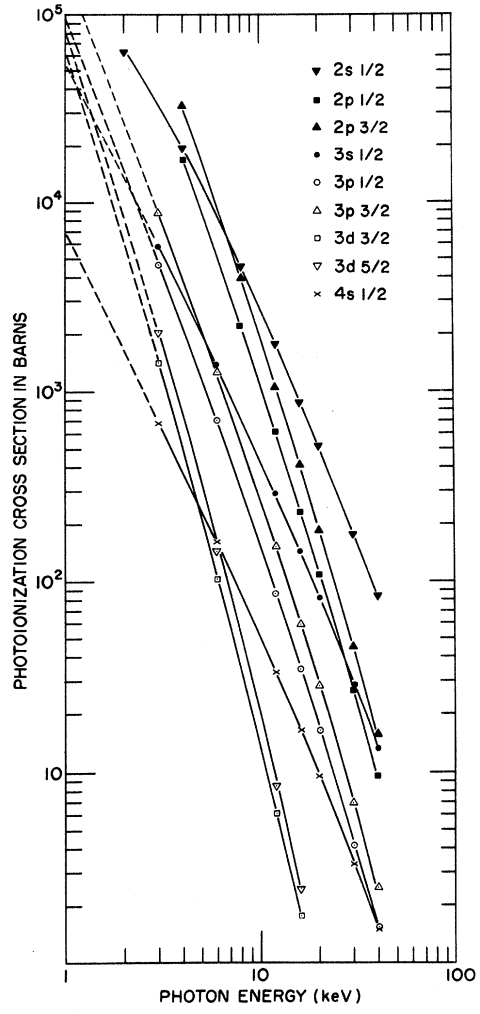

FIG. 4. Calculated partial photoionization cross sections for the different indicated sublevels of krypton as a function of the photon energy. These calculations were performed by Ron using the method described in Ref. 15. The points shown on each curve indicate energies at which numbers were actually obtained. The dashed portions of each curve are extrapolations.

values used for the α_{2s}^c's.

Ionization can occur from all electronic levels of argon with 5.4- and 8.0-keV x rays. Table V shows a comparison of the present 5.4-keV values with earlier experimental values[5] obtained with a titanium target (4.5 keV). Again, the theoretical values[5] are based on Auger processes and electron shakeoff. The agreement is better here, which is expected since the partial photoionization cross sections used by Carlson and Krause agree closely with those interpolated from Rakavy and Ron.[15]

In Table VI the data for krypton ionized by 0.28-keV x rays are compared with results in which the most probable photon energy was assumed to also be 0.28 keV.[7] Although the two results agree within the quoted uncertainties, the higher charge states are somewhat more abundant for the present experiment, which is particularly noticeable for Kr^{+2} and Kr^{+3}. This can possibly be explained by the difference in the character of the ionizing x rays. Our x-ray spectrum was essentially monoenergetic and could produce ionization in the $3p$ and $3d$ levels and in the $n=4$ level, whereas the relative probability for photoabsorption for the x-ray spectrum used in the previous experiment showed that about 20% of the ionization was produced by photons with only enough energy to ionize in the $3d$ and $n=4$ levels. According to a previous experiment,[7] if the photons are only energetic enough to ionize in the $3d$ level or $n=4$ level, then the Kr^{+2} is about twice as abundant as Kr^{+3}; thus the Kr^{+2} abundance would be enhanced by the contribution from low-energy x rays.

Ionization becomes possible in the $3s$ level of krypton when 1.5-keV x rays are used. Previous similarities in the relative abundances of ions produced by photons of different energies but which ionize from the same atomic levels suggest that these results should be compared with a previous experiment[7] in which the average photon energy was 1.15 keV (Table VI). However, in this case extrap-

TABLE VI. Relative abundance of krypton ions following ionization by 0.28- and 1.5-keV x rays. Comparisons with previous experiment and theory.

	0.28 keV			1.5 keV		
	Y_c/Y			Y_c/Y		
Charge of ion (c)	Uncorrected	Corrected (0.05 ± 0.01 eV)	Previous experiment[a]	Uncorrected	Corrected (0.05 ± 0.01 eV)	Previous experiment[b]
1	0.017 ± 0.003	0.025 ± 0.004	0.025 ± 0.006	0.032 ± 0.004	0.051 ± 0.005	0.03 ± 0.005
2	0.440 ± 0.010	0.470 ± 0.012	0.519 ± 0.005	0.162 ± 0.009	0.183 ± 0.011	0.275 ± 0.016
3	0.436 ± 0.010	0.411 ± 0.010	0.398 ± 0.006	0.372 ± 0.014	0.371 ± 0.015	0.408 ± 0.015
4	0.095 ± 0.005	0.084 ± 0.005	0.075 ± 0.003	0.273 ± 0.012	0.254 ± 0.012	0.229 ± 0.009
5	0.012 ± 0.004	0.010 ± 0.004	0.007 ± 0.002	0.120 ± 0.008	0.107 ± 0.008	0.072 ± 0.005
6				0.024 ± 0.005	0.021 ± 0.005	0.013 ± 0.005
7				0.015 ± 0.004	0.013 ± 0.004	

[a]Reference 7.

[b]Produced by x rays of average energy 1.15 keV (Ref. 7).

olated values from Ron's[16] calculated partial photoionization cross sections shown in Fig. 4 as well as values obtained by Krause[27] and by Cooper and Manson[28] indicate that the relative amounts of $3s$, $3p$, and $3d$ ionization vary over the energy range 1.15–1.5 keV in such a way that ionization from the $3s$ level decreases more slowly with increasing energy than ionization from the $3p$ and $3d$ levels. This would explain the difference in the ion spectra for the two experiments, since the increased relative probability for ionization in the $3s$ level at 1.5 keV would result in a greater percentage of higher charged ions. Because of this energy-dependent uncertainty in the cross sections, it is possible that the rearrangement probabilities are still energy independent.

The 5.4- and 8.0-keV x rays fall between the K and L levels in krypton. In Table VII, the 5.4-keV results are compared with a calculation and an experiment[7] in which the primary ionizing energy was 4.5 keV. There is a slight disagreement between the two experimental values which again is possibly due to the energy dependence of the partial photoionization cross sections (Fig. 4). The theoretical values at 5.4 and 8.0 keV were obtained using partial cross sections for krypton calculated by Ron[16] and shown in Fig. 4. The estimated uncertainty of the calculated values is 25%, and within this limit, the agreement between theory and experiment is adequate.

Although all of the data presented here generally agree where possible with previous results, there does seem in some cases to be a small but systematic shift in intensity toward the higher charged ions in our work. This could be due in part to the charge-dependent detector response mentioned earlier for which no correction was made.

IV. CONCLUSION

The relative abundances of multiply charged ions observed here are consistent with previous measurements and, except for neon at 0.28 keV, with theoretical predictions which take into account Auger transitions and electron shakeoff. The results again indicate that additional effects such as electron correlation must be included for neon.

TABLE VII. Relative abundance of krypton ions following ionization by 5.4- and 8.0-keV x rays. Comparison with theory and experiment.

	5.4 keV				8.0 keV		
	Y_c/Y				Y_c/Y		
Charge of ions (c)	Uncorrected	Corrected (0.05 ± 0.01 eV)	Previous experiment[a]	Theory[a]	Uncorrected	Corrected (0.05 ± 0.01 eV)	Theory[b]
1	0.016 ± 0.008	0.028 ± 0.010	0.013 ± 0.006	0.004	0.023 ± 0.009	0.040 ± 0.009	0.001
2	0.011 ± 0.003	0.014 ± 0.005	0.033 ± 0.006	0.027	0.016 ± 0.006	0.020 ± 0.008	0.023
3	0.057 ± 0.005	0.064 ± 0.006	0.073 ± 0.006	0.073	0.040 ± 0.012	0.044 ± 0.013	0.072
4	0.170 ± 0.010	0.177 ± 0.011	0.209 ± 0.009	0.227	0.183 ± 0.021	0.189 ± 0.022	0.210
5	0.217 ± 0.011	0.216 ± 0.012	0.233 ± 0.009	0.234	0.195 ± 0.022	0.193 ± 0.023	0.208
6	0.245 ± 0.012	0.236 ± 0.013	0.225 ± 0.011	0.194	0.268 ± 0.026	0.257 ± 0.026	0.200
7	0.206 ± 0.010	0.194 ± 0.010	0.152 ± 0.008	0.159	0.180 ± 0.022	0.169 ± 0.022	0.179
8	0.065 ± 0.005	0.060 ± 0.005	0.052 ± 0.005	0.073	0.083 ± 0.013	0.076 ± 0.013	0.085
9	0.012 ± 0.003	0.011 ± 0.003	0.010 ± 0.003	0.007	0.011 ± 0.006	0.010 ± 0.006	0.008
10	0.0005 ± 0.0009	0.0005 ± 0.0009		0.0015	0.002 ± 0.002	0.002 ± 0.002	0.002

[a]Using x rays of average energy 4.5 keV (Ref. 7).

[b]Obtained with α_i^c's from Ref. 7 and σ_i's from Ref. 16.

Our results, when interpreted in terms of partial photoionization cross sections calculated by Rakavy and Ron, [15] indicate that the previous disagreement between theory and experiment for argon L-shell ionization is possibly due to a poor choice of partial photoionization cross sections. Small discrepancies between the measured relative abundances of krypton ions can also be explained in terms of the energy dependence of the partial photoionization cross sections predicted by Ron. [16] Within the uncertainties of the data there was no evidence for an energy dependence for the rearrangement probabilities (α_i^c's), following inner-shell ionization in the energy range for which the sudden approximation used to predict electron shakeoff is valid. [2,11]

ACKNOWLEDGMENTS

The authors wish to express their appreciation for the contributions to this work by Dr. S. K. Kahng and Dr. H. S. Landes in the design and construction of the TOF mass spectrometer, and to Dr. A. Ron for providing the calculated partial photoionization cross sections for krypton.

---

*Research supported by the Aerospace Research Laboratories, Office of Aerospace Research, U. S. Air Force, under Contract No. F-33615-69-C-1048.

†Present address: Westminster College, New Wilmington, Penn. 16142.

[1]P. Auger, J. Phys. Radium 6, 205 (1925).

[2]M. O. Krause, M. L. Vestal, and W. H. Johnston, Phys. Rev. 133, A385 (1964).

[3]T. A. Carlson and M. O. Krause, Phys. Rev. Letters 14, 390 (1965).

[4]T. A. Carlson, Phys. Rev. 156, 142 (1967).

[5]T. A. Carlson and M. O. Krause, Phys. Rev. 140, A1057 (1965); 137, A1655 (1965).

[6]T. A. Carlson, Phys. Rev. 130, 2361 (1963).

[7]M. O. Krause and T. A. Carlson, Phys. Rev. 149, 52 (1966); 158, 18 (1967).

[8]T. A. Carlson and M. O. Krause, Phys. Rev. Letters 17, 1079 (1966).

[9]M. O. Krause, T. A. Carlson, and R. D. Dismukes, Phys. Rev. 170, 37 (1968).

[10]T. A. Carlson, W. E. Moddeman, and M. O. Krause, Phys. Rev. A 1, 1406 (1970).

[11]E. L. Feinberg, J. Phys. (USSR) 5, 423 (1941); A. Migdal, J. Phys. (USSR) 4, 449 (1941). First proposed to explain ionization following inner-shell vacancies created by nucleon decay.

[12]F. W. Bryon and C. J. Joachain, Phys. Rev. 164, 1 (1967).

[13]R. L. Brown, Phys. Rev. A 1, 586 (1970).

[14]Tu-Nan Chang, T. Ishihara, and R. T. Poe, Bull. Am. Phys. Soc. 16, 126 (1971).

[15]G. Rakavy and A. Ron, Phys. Rev. 159, 50 (1967).

[16]A. Ron (private communication). Cross sections for krypton have been calculated for selected energies from 1.0 to 40 keV using the method described in Ref. 15. The results are shown in Fig. 4.

[17]P. A. Ross, Phys. Rev. 28, 425A (1926).

[18]The mass absorption coefficients used to compute the filter transmission were from B. L. Henke, R. L. Elgin, R. E. Lent, and R. B. Ledinghan, Norelco Reptr. 14, 112 (1967), and tables complied by N. V. Philips Gloeilampenfabrieken, Eindhoven, Holland which appeared as a supplementary insertion in Norelco Reptr. 9, (1962).

[19]W. C. Wiley and I. H. McLaren, Rev. Sci. Instr. 26, 1150 (1955).

[20]S. K. Kahng, thesis (University of Virginia, 1967) (unpublished).

[21]R. J. Van Brunt, G. S. Lightner, and W. D. Whitehead, Rev. Sci. Instr. (to be published).

[22]G. S. Lightner, thesis (University of Virginia, 1971) (unpublished).

[23]W. W. Hunt, K. E. McGee, J. K. Streeter, and M. S. Maughan, Rev. Sci. Instr. 49, 1793 (1968).

[24]A similar dependence was observed with a different type of electron multiplier by B. L. Schram, A. J. H. Berboom, and J. Kistermaker, Physica 32, 185 (1966); B. L. Schram, *ibid.* 32, 197 (1966).

[25]A. P. Lukirskii, T. M. Zimkina, and I. A. Brytov, Bull. Acad. Sci. USSR Phys. Ser. 27, 808 (1963).

[26]A. J. Bearden, J. Appl. Phys. 37, 1689 (1966).

[27]M. O. Krause, Phys. Rev. 177, 151 (1969).

[28]J. W. Cooper and S. T. Manson, Phys. Rev. 177, 157 (1969).